Comparison of Thermodynamic Databases for 3xx and 6xxx Aluminum Alloys

C. RAVI and C. WOLVERTON

Computational thermodynamics, or Calculation of Phase Diagram (CALPHAD) methods have proven useful in applications to modeling a variety of alloy properties. However, the methods are only as accurate as the thermodynamic databases they use, and two commercial thermodynamic databases exist for aluminum alloys: Thermotech and Computherm. In order to provide a critical comparison of these databases, we used both the databases to calculate equilibrium solid-state phase fractions and phase diagram isothermal sections of several industrial aluminum alloys: a 319-type and 356 cast alloys, as well as the wrought alloys 6022 and 6111. All of these alloys may be generically described as being based on the Al-Mg-Si-Cu quaternary with other additions such as Fe, Mn, and Zn. Although many of the results are consistent between the two databases, several qualitative and quantitative differences were observed. Many of these differences are found to be due to the intermetallic compounds involving Fe, Mn, Cr, and Zn. On the other hand, thermodynamics involving only phases from the Al-Mg-Si-Cu quaternary show good agreement between the databases, although some small differences still exist, particularly involving the quaternary Q phase. To understand and assess these differences, formation enthalpies and reaction energies from the databases were compared against density functional first-principles energetics. These comparisons indicate possible avenues for future improvements of Al-alloy thermodynamic databases. Finally, we demonstrate an interesting correlation between the calculated phase fractions and the measured yield strengths across this wide family of 3xx cast and 6xxx wrought alloys.

I. INTRODUCTION—COMPUTATIONAL THERMODYNAMICS DATABASES

COMPUTATIONAL thermodynamics approaches[1] have been widely used and highly successful in predicting phase equilibria in complex, multicomponent, industrial alloys. These approaches are also often referred to as Calculation of PHAse Diagram (CALPHAD) methods. The considerable significance of CALPHAD modeling is reflected in the large number of recent related research publications.[2–15] CALPHAD methods have also recently been used in many industrial problems, such as several studies of cast A1319-type alloys: (1) the simulation of solidification in A1319;[2] (2) obtaining an improved equilibrium and metastable Al-Cu phase diagram, incorporating a first-principles description of the strengthening precipitate Al_2Cu (θ'), which is otherwise missing from the thermodynamic databases;[3] (3) providing Al_2Cu (θ') precipitate phase fraction information for constructing a predictive model of thermal growth of A1319 during heat treatment;[4] and modeling the age-hardening behavior of A1319 alloys.[5]

CALPHAD methods rely on databases of thermodynamic functions, obtained from an optimization process involving experimental thermodynamic data combined with observed phase diagrams. Given the thermodynamic database, the CALPHAD programs perform minimization of the multicomponent free-energy functional of interest to predict phase equilibria. The advantage of these methods is that phase equilibria in industrial, multicomponent materials (sometimes consisting of a dozen components) can be extrapolated from databases of thermodynamic information on unary, binary, and ternary (and some quaternary) phases. However, these computational thermodynamics methods cannot predict the existence of new phases, but rather can only minimize free energies with respect to the proportions of phases that exist in the database. Although the computational thermodynamics programs have been used extensively for solidification simulations,[16] application of these methods to solid-state phase equilibria in industrial alloys is far less typical. Knowledge of solid-state phase equilibria is an important factor in determining the type, size, morphology, and distributions of phases and precipitates present in alloys, often controlling factors in mechanical properties.[4,5,17] Hence, we focus our study generally on solid-state phase equilibria, and specifically on several 3xx and 6xxx aluminum alloys of industrial interest.

For aluminum alloys, we consider two existing commercial thermodynamic databases: (1) one from ThermoTech[18] and (2) another from CompuTherm LLC.[19] In this article, we will refer to these two databases as "Thermotech" and "Computherm," respectively. In order to compare the two databases, we performed calculations of equilibrium solid-state phase fractions and isothermal phase diagram sections of several industrial aluminum alloys. PANDAT software was used for all of the calculations presented here.[20] It should be noted that the lists of phases included in the Thermotech/Computherm databases are not identical. Thus, qualitative differences in the predicted phase fractions between the two databases can be due to differences in the thermodynamic functions in the

---

C. RAVI, Postdoctoral Research Scientist, formerly with Ford Research and Advanced Engineering, Department of Materials Science and Engineering, The Pennsylvania State University, University Park, PA 16802, is with the Institute of Mathematical Science, CIT Campus, Chennai 600 113, India. Contact e-mail: ravic@imsc.res.in C. WOLVERTON, Research Scientist, is with Ford Research and Advanced Engineering, Ford Motor Company, Dearborn, MI 48121.

Manuscript submitted January 4, 2005.

databases, or can be due to the relative presence/absence of a phase in one database, but not the other.

II. ALLOYS FOR STUDY

The advantages of weight reduction, fuel savings, and reduced emissions associated with the use of lightweight aluminum alloys has motivated the consideration of their increased use in the automotive industry. Cast alloys in the 3xx (Al-Si) class based on the Al-Si-Mg (*e.g.*, 356) and Al-Si-Cu (*e.g.*, 319) systems are widely used in various automotive applications, such as engine blocks and cylinder heads, wheels, chassis components, and gear housings.[21] For body panel applications, the wrought heat-treatable 6xxx alloys, based on Al-Mg-Si-(Cu), are being evaluated to replace steel.[21] These current and future applications of Al alloys in turn require stringent characterization of physical and mechanical properties of these materials.[22] Hence, for the comparison of the thermodynamic databases, we chose to examine the phase stability of the following alloys: (1) a 319-type alloy, (2) 356, (3) 6022, and (4) 6111.

It should be noted that all these alloys share some common characteristics: they are all based on the Al-Mg-Si-Cu quaternary system and they are all heat treatable and high-strength aluminum alloys. The chemical compositions of the alloys used in the calculations are given in Table I. We also note that the alloys typically contain Fe, the presence of which gives rise to various intermetallic phases (*e.g.* Al-Fe-Si phases), which are generally detrimental to mechanical properties.[23] The Mn and Cr are often added to alter the morphology and types of these Fe-containing intermetallic phases, at least partly ameliorating their negative effects.

III. RESULTS—CALCULATED EQUILIBRIUM PHASE FRACTIONS

For each alloy, the stable phases and equilibrium phase fractions were calculated from each database over the temperature range of 0 °C to 700 °C. Unless specifically noted, all phases in each database were included in the free-energy minimization for each calculation. We next discuss these results for each alloy.

A. *W319 Alloy*

W319 (a slight variation of AA319) is an Al-Si-Cu-(Mg) casting alloy. W319 contains relatively large alloying additions of Si and Cu compared to Mg. We begin with this alloy because it has been extensively studied, and the various phases present in cast W319 have been experimentally identified.[5,24] In Figure 1, we show the calculated equilibrium phase fractions. The left side panels (a) and (b) show the phase fractions of all the phases (except Al) obtained with the two databases. Because of the relatively large Si fraction we have given a detailed view (c) and (d) of the low-fraction (less than about 2 wt pct) phases separately on the right side panels. We summarize our observations regarding the two thermodynamic databases as follows. (1) As seen in Figure 1, both the databases show that Si is the predominant phase, and Al_2Cu with the next largest phase fraction. The quaternary Q and Fe-containing α-AlFeMnSi phases are also observed with both the databases. We note here that the transmission electron microscopy (TEM) experimental observation of phases[23] in this alloy shows the presence of the following phases: Al, Si, Al_2Cu, Q, α-AlFeMnSi, and β-AlFeSi. Both databases correctly predict the qualitative presence of Al, Si, Al_2Cu, and Q phases, whereas there are differences in the predicted Fe-containing phases between Thermotech and Computherm. (2) With respect to the equilibrium phase fraction of Al_2Cu, a major quantitative difference between the two databases is observed (Figure 1). The phase fraction obtained using the Thermotech database shows a steady increase as the temperature of the alloy is decreased. However, the phase fraction obtained using the Computherm database reaches a maximum as the temperature of the alloy decreases to about 240 °C, and then it decreases to a lower value as the temperature is lowered further. This low-temperature abrupt decrease in the Al_2Cu phase fraction corresponds to the appearance of the τ-AlCuZn phase in the Computherm result, a phase that is not present in the Thermotech database. (3) Results based on the Thermotech database show that the dominant Fe/Mn-containing phase is α-AlFeMnSi, whereas with the Computherm database, together with α-AlFeMnSi, two other phases, $Al_{12}Mn$ and β-AlFeSi, are observed. Very small fractions of $Al_{13}Cr_4Si_4$ and Al_3Ti are observed from Thermotech, but these phases are not present in the Computherm database. (4) Differences due to the presence/absence of Al_3Ti, $Al_{13}Cr_4Si_4$, $Al_{12}Mn$, and τ-AlCuZn phases are due to the fact that these phases are present in one of the databases, but absent in the other. However, β-AlFeSi is contained in both databases, so its presence in Computherm, but not Thermotech, results is presumably due to the differences in the thermodynamic functions of this and other competing phases.

Table I. Chemical Composition of the Alloys Considered in This Study (Weight Percent)

Element	W319	356	6022	6111
Al	bal	bal	bal	bal
Mg	0.30	0.28	0.58	0.75
Si	7.50	6.72	1.28	0.63
Cu	3.50	0.10	0.07	0.75
Mn	0.25	0.00	0.08	0.05
Fe	0.30	0.10	0.11	0.05
Ti	0.13	0.12	0.00	0.06
Zn	0.22	0.00	0.00	0.00
Cr	0.02	0.00	0.00	0.06

B. *356 Alloy*

Relative to W319, we see from Table I that the composition of 356 contains little Cu, and does not include Mn, Cr, and Zn. The Fe content is also relatively low. The calculated equilibrium phase fractions in the cast alloy 356 are shown in Figure 2. We note that other than Si, all the phases predicted in 356 have fairly low phase fractions (less than 1 wt pct). Both the databases show Si, Q, $Al_8FeMg_3Si_6$, and β-AlFeSi phases. Interestingly, both databases predict $Al_8FeMg_3Si_6$, and β-AlFeSi phases. Interestingly, both databases predict $Al_8FeMg_3Si_6$ to be stable only over a narrow temperature window, and do not indicate that this is a low-temperature ground state of this alloy. There is generally

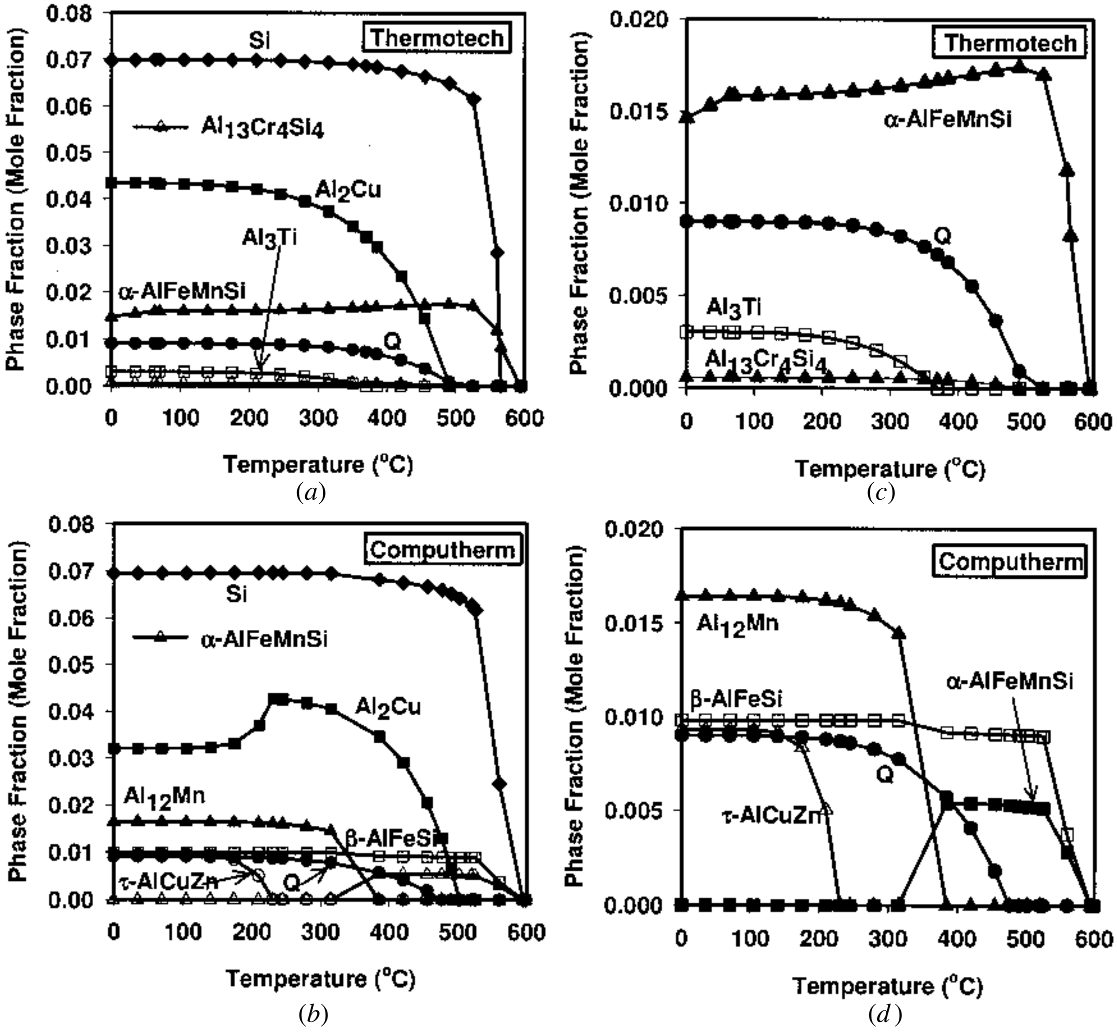

Fig. 1—Calculated equilibrium phase fractions in W319 with the (*a*) and (*c*) Thermotech and (*b*) and (*d*) Computherm databases. (a) and (b) show the phase fraction of all the phases (except Al), and (c) and (d) give a detailed view of the low-fraction phases.

good agreement between the two databases for not only the qualitative phases but also the quantitative phase fractions in this alloy. Since many of the differences between the databases observed previously in the W319 seem to be due to the Fe/Mn containing phases, the overall better agreement in the case of 356 could be related to the relatively small amount of these elements in this alloy. We investigate this idea further in Section C. As with W319, we also note the difference that Thermotech shows a small amount of Al_3Ti to be stable, whereas it is absent in Computherm database.

C. *6022 Alloy*

The wrought 6xxx series alloy chemistries can be distinguished from the cast alloys by the much lower levels of Si in the wrought alloys. Nevertheless, Si is still a major alloying element in 6xxx aluminum alloys, as is Mg (Table I). Figure 3 shows the calculated equilibrium phase fractions in a 6022 alloy obtained using both the Thermotech and Computherm databases. It is evident from Figure 3 that both the databases show Si and Mg_2Si are the most predominant phases with nearly equal phase fractions. The *Q* phase is also predicted to be stable with very similar phase fractions between the two databases. The notable differences are as follows. (1) Over the temperature window 400 °C to 550 °C, the $Al_8FeMg_3Si_6$ phase is stable in the Computherm calculation, but not in Thermotech. This difference is interesting, since in 356, $Al_8FeMg_3Si_6$ is stable in both databases. (2) At 400 °C, the phase fractions of Si and Mg_2Si change continuously in the results with Thermotech, whereas these phases show an abrupt drop at this temperature with the Computherm database. The abrupt drop corresponds to the appearance of the (Mg- and Si-containing) $Al_8FeMg_3Si_6$ phase at this temperature. (3) As with the cast alloys, relatively large fractions of $Al_{12}Mn$ and β-AlFeSi are observed in the Computherm results, whereas the corresponding phase in the Thermotech results is the α-AlFeMnSi. Note that a small amount of β-AlFeSi is predicted to be stable in the Thermotech calculations at low temperature.

D. *6111 Alloy*

The wrought age hardening 6111 alloy has an enhanced amount of Cu, and reduced Si content in relation to 6022 (Table I). The computed equilibrium phase fractions in 6111 are plotted in Figure 4. Both the databases show *Q* as the dominant phase, and Al_2Cu as the next most dominant phase. It is interesting to note the interplay between the Mg_2Si, *Q*,

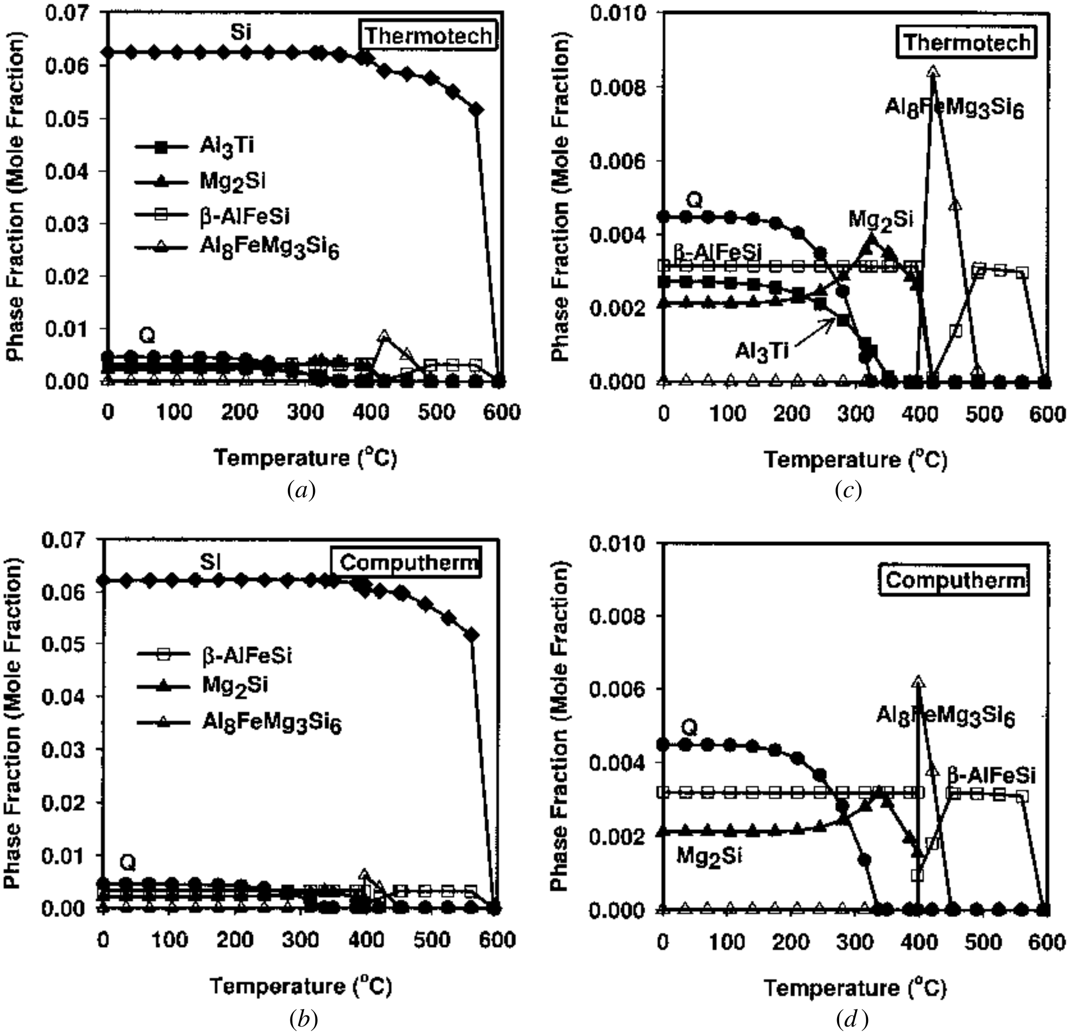

Fig. 2—Calculated equilibrium phase fractions in 356 with the (*a*) and (*c*) Thermotech and (*b*) and (*d*) Computherm databases. (a) and (b) show the phase fraction of all phases (except Al) and (c) and (d) give a detailed view of the low-fraction phases.

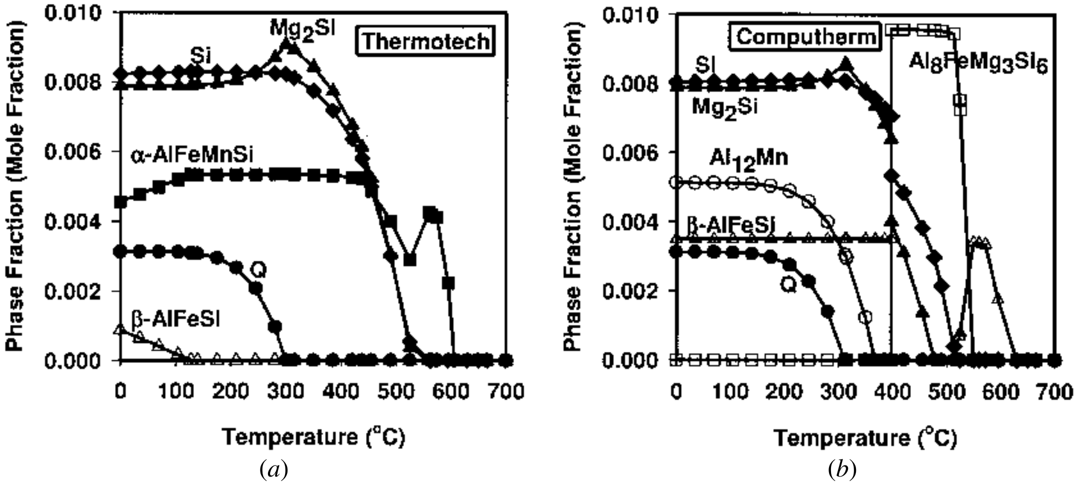

Fig. 3—Calculated equilibrium phase fractions in 6022 using (*a*) Thermotech and (*b*) Computherm databases. Shown are phase fractions of all the phases except Al.

and Al_2Cu phases. Starting at high temperature and coming down, first, the Mg_2Si phase appears and begins to increase in fraction until a temperature is reached, at which time the *Q* phase becomes stable. At this point, Mg_2Si decreases in favor of *Q*. However, as the temperature is lowered further, eventually Al_2Cu becomes stable, and then the *Q* phase

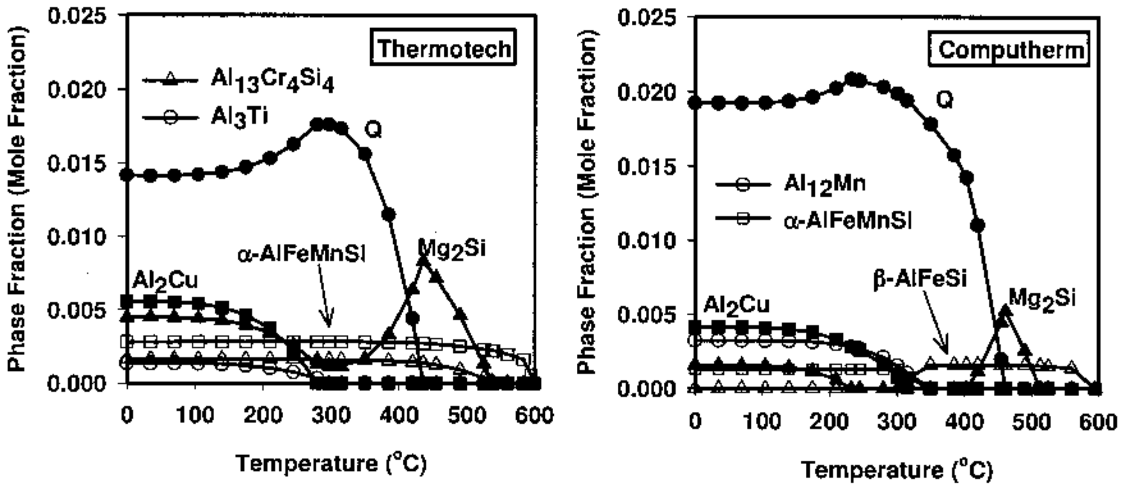

(*a*) (*b*)

Fig. 4—Calculated equilibrium phase fractions in 6111 using the (*a*) Thermotech and (*b*) Computherm databases. Shown are phase fractions of all the phases except Al.

decreases in favor of both Al_2Cu and Mg_2Si. This nonmonotonic behavior of the phase fractions of Mg_2Si and Q is consistently predicted by both databases. We also note the following differences. (1) There are quantitative differences in the predicted fractions of Q and Al_2Cu (θ) phases. (2) As seen in the other alloys, Al_3Ti and $Al_{13}Cr_4Si_4$ are present in the Thermotech database, which are absent in the Computherm database, and *vice versa* with respect to the $Al_{12}Mn$ phase.

E. *Isolating the Discrepancies between the Databases: Eliminating the "Suspicious" Phases*

We have seen in Section III A-D that the intermetallic compounds (*e.g.*, $Al_{13}Cr_4Si_4$, $Al_{12}Mn$, α-AlFeMnSi, and β-AlFeSi) involving Cr/Mn/Fe are largely responsible for the differences between the results based on the Thermotech and Computherm databases. Since some of these phases as well as others (*e.g.*, τ-AlCuZn and Al_3Ti) are present in one database but absent in the other, our comparisons of the thermodynamic descriptions are somewhat ambiguous.

To facilitate a more direct comparison of the thermodynamic functions present in the databases, additional calculations of equilibrium phase fractions were performed for W319 and 356, including only a limited number of phases in the calculations. In each case, we have eliminated the "suspicious" phases ($Al_{13}Cr_4Si_4$, $Al_{12}Mn$, α-AlFeMnSi, β-AlFeSi, τ-AlCuZn, and Al_3Ti), which seem to be the source of the discrepancy, and repeated the calculations for the cast Al alloys, including only phases in the Al-Mg-Si-Cu quaternary (Al, Si, Mg_2Si, Al_2Cu, and Q).

Equilibrium phase fractions based on calculations including only these limited phases from the databases for each of the cast alloys are plotted in Figure 5. We see that for these calculations involving only Al-Mg-Si-Cu intermetallic phases, both databases produce very similar phase fractions. (We do note, though, that the phase fraction calculations of Q in the 6111 alloys indicate some quantitative distinction between the databases, even for this quaternary system. We return to this issue in Section IV.) Thus, we assert that the main source of discrepancy between the Thermotech and Computherm databases lies in the differences of thermodynamic data for the Cr/Mn/Fe-containing intermetallic phases, as well as cases of phases included in one database but not the other (*e.g.*, $Al_{12}Mn$, τ-AlCuZn in Computherm and $Al_{13}Cr_4Si_4$ and Al_3Ti in Thermotech). A future re-evaluation of the thermodynamics of the Al-Fe-Mn-Si system would therefore be of considerable interest, as would the inclusion of these missing phases in each database.

IV. RESULTS—CALCULATED SOLID-STATE ISOTHERMAL SECTIONS

The compositions of the alloys listed in Table I are only representative chemistries; in practice, the alloying elements always have defined acceptable compositional ranges. To investigate the influence of alloy composition on the equilibrium phases, we have also computed low-temperature isothermal sections of Al-Mg-Si-Cu quaternary alloys with a fixed Si content and varying concentrations of Mg and Cu. The isothermal sections are calculated for 7 wt pct and 1 wt pct Si, to generically represent the composition space for the cast and wrought Al alloys, respectively.

The isothermal sections calculated at 250 °C are shown in Figures 6 and 7. Figure 6 gives the isothermal section for 7 wt pct Si, and indicates the compositional ranges of the cast alloys 319 and 356. Figure 7 gives the isothermal section for 1 wt pct Si, and the dashed-line boundary is for the generic composition field of 6xxx alloys.[25]

Although the isothermal sections obtained using the two databases do have the same phase diagram topology, the Si + Q phase field is slightly wider in Thermotech relative to Computherm in both Figures 6 and 7. Also, we note that in Figure 6, alloy 356 falls very close to the phase boundaries between the stability regions Si + Q + Al_2Cu, Si + Q, and Si + Q + Mg_2Si. Thus, even the small differences in phase boundaries can have a significant effect on the alloy. It should further be noted that the compositional range for 356 alloys overlaps all three of these regions (in the Thermotech calculations), so depending on the Mg and Cu content of these alloys, one can form (in addition to Si and Q) either Al_2Cu, or Mg_2Si, or neither.

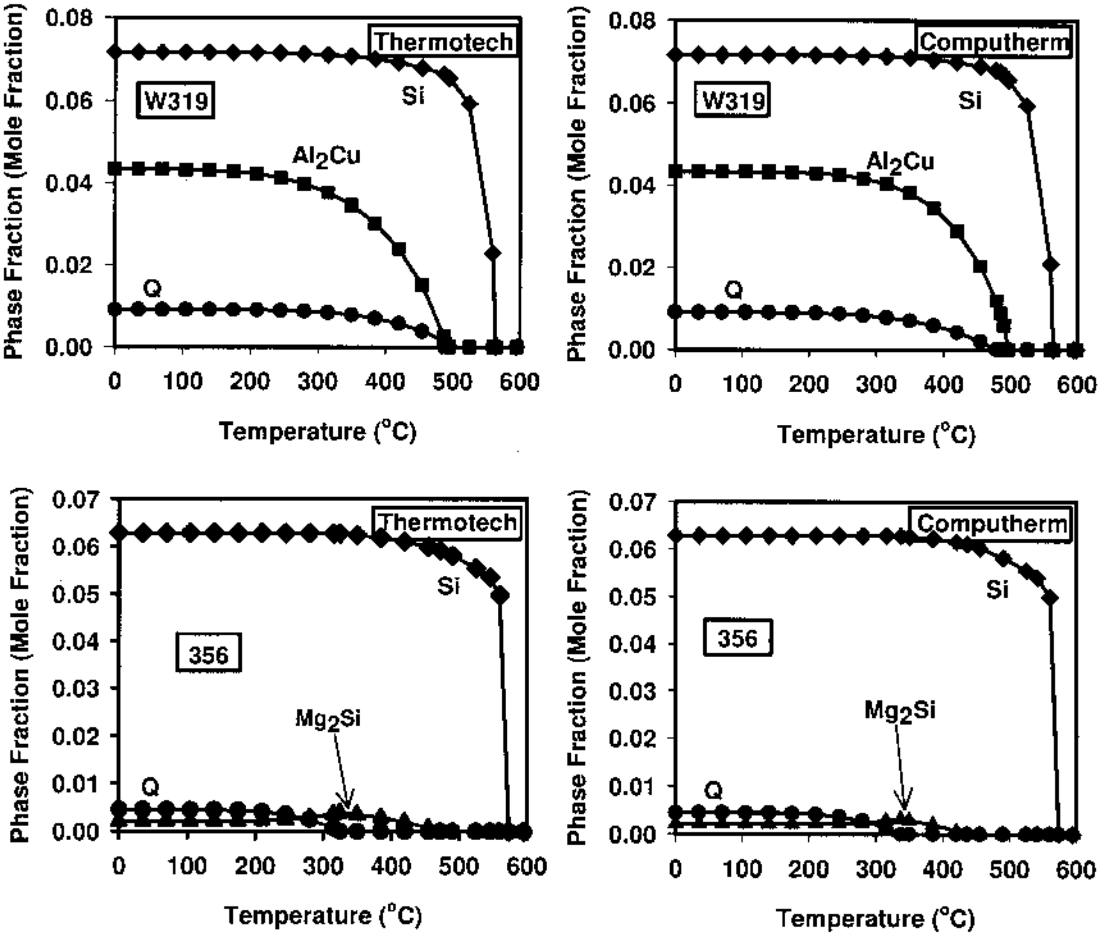

Fig. 5—Equilibrium phase fractions in W319 and 356 based on calculations including only limited phases from each of the databases. In each case, only phases in the Al-Cu-Mg-Si quaternary (Al, Si, Al_2Cu, Mg_2Si, and Q) are included.

From Figure 7, we note that the composition range for the 6xxx class also overlaps these stability regions, and so one can form Al_2Cu or Mg_2Si in 6xxx alloys, but *Q* is always predicted to be present. We also note that the difference in width of the Si + *Q* field makes 6111 fall quite close to the Si + Q + Al_2Cu/Si + Q boundary in the Thermotech calculation, but farther away from the boundary in the Computherm calculation. Thus, although the descriptions of the Al-Mg-Si-Cu quaternary are similar in Thermotech and Computherm, there are some subtle differences in the descriptions of the *Q* phase relative to Al_2Cu + Mg_2Si that have emerged in Figure 6 and 7. Since some alloy compositions are quite sensitive to the relative competition between Q, Al_2Cu, and Mg_2Si, we investigate the relative stability of these phases in more depth. We show next that first-principles atomistic calculations provide a means to predict the energetics of these and other phases, and hence can be used to discriminate between the two databases.

V. RESULTS—FIRST-PRINCIPLES ENERGETICS AS A DISCRIMINATOR OF EXISTING DATABASES

In order to help differentiate between the two thermodynamic databases, we need an independent, accurate source of thermodynamic information. To that end, we have performed density functional theory based first-principles calculations of (zero-temperature) energetics of several of the relevant intermetallic compounds discussed previously. These first-principles energetics have been shown (*e.g.*, Reference 3) to provide accurate formation enthalpies of Al intermetallics, relative to experimental or CALPHAD values. Our first-principles calculations employ the Vienna *Ab initio* Simulation Program[26] (VASP) in both the local density approximation[27] (LDA) and the generalized gradient approximation[28] (GGA) for the exchange correlation with the ultrasoft pseudopotentials. Details of *k*-point meshes and plane wave energy cutoffs are given subsequently. In all cases, structures are fully relaxed to their zero-force (or zero-stress) positions with respect to all cell-internal and cell-external degrees of freedom allowed by symmetry.

To compare with the thermodynamics databases, we have computed the $T = 0$K formation enthalpies, ΔH, of each of these phases using first-principles density functional calculations. The formation enthalpy of a compound σ is defined as

$$\Delta H(\sigma) = E(\sigma) - \sum_i x_i E_i \qquad [1]$$

where $E(\sigma)$ is the total energy of the compound, x_i is the fraction of the element i in the compound, and E_i is the energy of the pure element i in its equilibrium reference state. For our calculations, we have used the following pure element

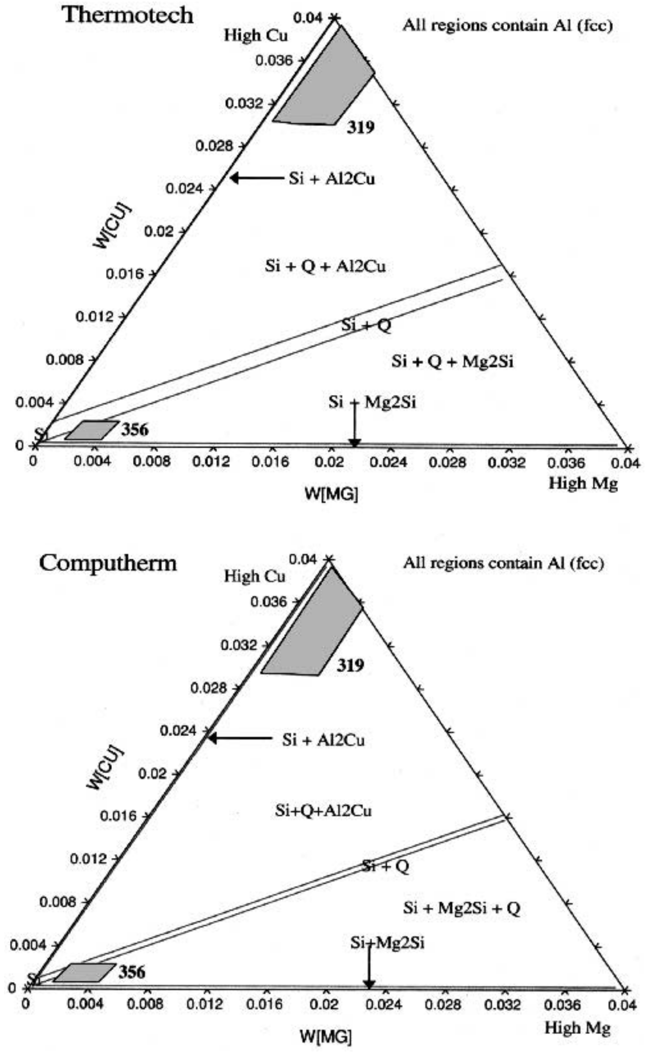

Fig. 6—Calculated isothermal section of Al-Mg-Si-Cu alloys at 250 °C with Al-7 wt pct Si. Compositions of 319 and 356 alloys are indicated.

reference states: fcc-Al, fcc-Cu, hcp-Mg, diamond-Si, bcc-Cr, bcc-Fe, nonmagnetic fcc-Mn, and hcp-Zn. For bcc-Fe, ferromagnetic calculations were performed, and for bcc-Cr, we use an antiferromagnetic (CsCl-type) geometry. Calculations of compound phases involving the magnetic elements, Cr, Mn, or Fe, correspond to nonmagnetic, non-spin-polarized state.

A. *Energetic Competition and Stability of Al_2Cu, Mg_2Si, and Q Phases*

We start by examining the energetic data from the aluminum databases and from first principles for the stability of Q relative to $Mg_2Si + Al_2Cu$. For the first-principles VASP calculations of Al-Mg-Si-Cu compounds, we find convergence of ΔH is achieved with a plane wave cutoff of 175 eV for the Al-Mg-Si phases and a 255 eV for the Cu-containing phases with a $(12 \times 12 \times 12)$ Monkhorst–Pack k-point mesh. Further information on crystal structures and phase stability for Al_2Cu, Mg_2Si, and Q phases can be found in our recent articles.[3,29,30]

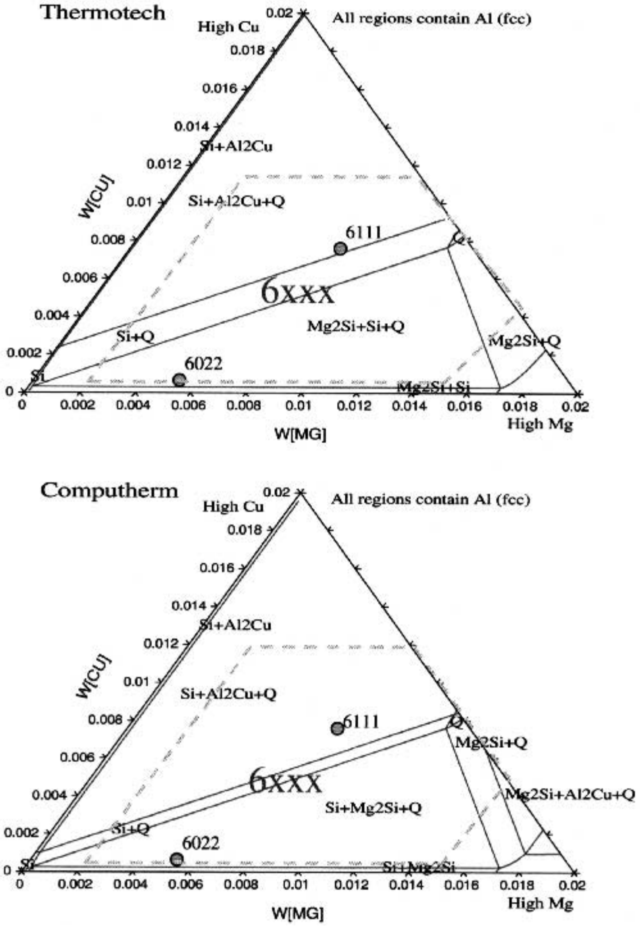

Fig. 7—Calculated isothermal section of Al-Mg-Si-Cu alloys at 250 °C with Al-1 wt pct Si. Composition ranges of 6xxx alloys are indicated.

In Table II, we list ΔH of Q, β-Mg_2Si, and θ-Al_2Cu (and several other phases, described in Section B) obtained from the CALPHAD databases (at $T = 270$ K), from our first-principles calculations (at $T = 0$K), and from experimental measurements, where available. From the results of this table, we note the following. (1) Comparison of the LDA and GGA first-principles numbers shows that LDA nearly always gives a more negative ΔH than GGA. This observation is interesting, since it is well known that LDA tends to "overbind," in the sense that LDA-predicted lattice parameters are smaller than experimental values, and LDA-predicted cohesive energies of solids typically are larger than experimental values. However, we know of no such well-known rule regarding the LDA prediction of ΔH. Although our calculations are only for a few compounds, we see that LDA tends to "overbind" also for ΔH values. (2) Comparison of first-principles values with the experimental values for θ and β shows the first-principles values to be quantitatively accurate to within roughly 10 pct. The GGA consistently seems to perform better than LDA, so for the remainder of the discussion, we consider the GGA results to be the most accurate prediction from first principles. Focusing the first-principles discussion to the GGA values will aid in providing predictions for phases for which no experimental data exist. (3) Comparison between GGA and CALPHAD results for θ and β shows a good agreement. However, this agreement is not terribly surprising, since the CALPHAD assessments have likely used the experimental values in their fitting procedures,

Table II. Formation Enthalpies (meV/Atom) for Several of the Intermetallic Phases Stable in the Al Alloys Considered Here*

		Formation Enthalpy, ΔH (meV/Atom)				
		CALPHAD		VASP		
Phase	Stoichiometry	Thermotech	Computherm	LDA	GGA	Experiment
θ	Al_2Cu	-159	-157	-185	-166	-164[32]
β	Mg_2Si	-218	-208	-175	-186	-218 ± 26[33]
Q	$Al_3Cu_2Mg_9Si_7$			-189	-175	
Q	$Al_5Cu_2Mg_8Si_6$	-182	-169	-146	-134	
$Al_{12}Mn$	$Al_{12}Mn$		-80	-101	-63	
$Al_{13}Cr_4Si_4$	$Al_{13}Cr_4Si_4$	-207		-211	-194	
π	$Al_8FeMg_3Si_6$	-117	-117	-24	$+24$	
T' (τ)	$Al_5Cu_4Zn_1$		-230	-69	-55	
	$Al_4Cu_4Zn_1\square^F$			-190	-171	

*Included are both the enthalpies from the CALPHAD computational thermodynamics databases (both Computherm and Thermotech) as well as the first-principles calculated values of the present work. First-principles values are calculated from VASP using both the LDA and the GGA.

and we have already seen the good agreement between GGA and experiment. (4) The Q phase represents an interesting story, due to its stoichiometry. The experimental determination of the stoichiometry and crystal structure of this phase is often ambiguous with respect to the precise Al/Mg/Si ratio in the structure. While the CALPHAD databases use $Al_5Cu_2Mg_8Si_6$ as the assumed stoichiometry of this phase, recent first-principles[31] work has shown that the $Al_3Cu_2Mg_9Si_7$ stoichiometry actually has the lowest energy. However, first-principles calculations can predict the energetics of not only the lowest-energy stoichiometry ($Al_3Cu_2Mg_9Si_7$), but also the commonly used $Al_5Cu_2Mg_8Si_6$ stoichiometry as well. Both are shown in Table II, and one can see that the energetic penalty for this change in composition is fairly large. We note that the comparison between the lowest-energy first-principles value (-175 meV/atom — GGA) and the CALPHAD values (-182 and -169 meV/atom for Thermotech and Computherm, respectively) is very good, provided that the lowest-energy stoichiometry $Al_3Cu_2Mg_9Si_7$ is used in the first-principles calculations. Thus, we assert that the commonly used stoichiometry for Q could be in error. Therefore, an experimental re-examination of the stoichiometry of Q would be of interest, as would the inclusion of off-stoichiometry in the CALPHAD description of this phase. We see below that the use of this stoichiometry has some implications on the relative stability of Q *vs* $\theta + \beta$, and therefore could affect the CALPHAD predictions of stability of this phase. We also note that there is a larger difference between the two databases for the Q phase than is typical for other phases, and the most accurate first-principles value falls somewhere intermediate between the two databases.

We also wish to compute the energetics of the competition of Q relative to β-Mg_2Si + θ-Al_2Cu. However, this issue is complicated by the various stoichiometries used for the Q phase. Hence, we have computed energies (δE_R) for several reactions of Q decomposing into Mg_2Si, Al_2Cu, Si, and Al:

I. $Al + Al_3Cu_2Mg_9Si_7 \rightarrow 2\ Al_2Cu + 9/2\ Mg_2Si + 5/2\ Si$
II. $Al_4Cu_2Mg_8Si_7 \rightarrow 2\ Al_2Cu + 4\ Mg_2Si + 3\ Si$
III. $Al_5Cu_2Mg_8Si_6 \rightarrow 2\ Al_2Cu + 4\ Mg_2Si + 2\ Si + Al$

The results are given in Table III. A positive value for the reaction energy indicates that Q phase is stable with respect to decomposition into Al_2Cu, Mg_2Si, and Si/Al. It should be noted that because the CALPHAD description of Q is based on composition $Al_5Cu_2Mg_8Si_6$, we could only compute the energy of Reaction III from CALPHAD, whereas the first-principles reaction energies correspond to each of the respective compositions of Q given in the reactions preceding. From the CALPHAD values in Table III, we see again that the Thermotech database predicts a more stable Q phase than Computherm, as we saw above in Figure 6 and 7. In addition, though, we see from the first-principles values that the stability of Q is strongly dependent on composition, and in going from the $Al_3Cu_2Mg_9Si_7$ to the $Al_5Cu_2Mg_8Si_6$ stoichiometry, the Q phase qualitatively changes from energetically stable to unstable. Probably the most reliable number in Table III is the GGA-calculated energy of Reaction I (+172 meV). It is interesting that this value is nearly intermediate between the two values from the CALPHAD databases: +250 and +105 meV for Thermotech and Computherm, respectively. Future refinements to these databases could be improved by incorporating this more accurate stability (and composition) of Q as predicted from first principles.

Table III. Comparison of CALPHAD (Computherm and Thermotech) and First-Principles (VASP) Reaction Energies Involving Decomposition of Q into θ, β, Si, and Al (meV/Formula Unit)*

	CALPHAD		VASP (FP)	
Reaction	Thermotech	Computherm	LDA	GGA
I			$+495$	$+172$
II			$+370$	$+21$
III	$+250$	$+105$	-155	-403

*The three reactions considered are as follows.
I. $Al + Al_3Cu_2Mg_9Si_7 \rightarrow 2\ Al_2Cu + 9/2\ Mg_2Si + 5/2\ Si$
II. $Al_4Cu_2Mg_8Si_7 \rightarrow 2\ Al_2Cu + 4\ Mg_2Si + 3\ Si$
III. $Al_5Cu_2Mg_8Si_6 \rightarrow 2\ Al_2Cu + 4\ Mg_2Si + 2\ Si + Al$
A positive energy implies Q is energetically stable with respect to this decomposition.

B. *First-Principles Energetics of $Al_{12}Mn$, $Al_{13}Cr_4Si_4$, π-$Al_8FeMg_3Si_6$, and τ-AlCuZn*

We have seen in Section III that the main source of discrepancy between the Thermotech and Computherm databases lies in the differences of thermodynamic data for the Cr/Mn/Fe-containing intermetallic phases, as well as cases of phases included in one database but not the other. Therefore, for each of the following phases, *viz.* $Al_{12}Mn$, $Al_{13}Cr_4Si_4$, π-$Al_8FeMg_3Si_6$, and τ-AlCuZn (or T′-$Al_4Cu_4Zn_1$), we extend comparison of the formation enthalpies from thermodynamic databases with their respective values from first-principles calculations. A systematic comparison of first-principles and CALPHAD stability of these phases should help to shed more light on the possible differences between predictions of the two CALPHAD databases. For the first-principles calculations of these four phases, total energy VASP calculations were performed with a plane wave energy cutoff of 350 eV. An $8 \times 8 \times 8$ ($10 \times 10 \times 10$) Monkhorst–Pack *k*-point mesh has been employed in the calculation of $Al_{13}Cr_4Si_4$ and T'-$Al_4Cu_4Zn_1$ ($Al_{12}Mn$ and π-$Al_8FeMg_3Si_6$).

Crystal structure information for each of these phases is listed in Table IV, along with calculated lattice parameters. We note that the crystal structure data for the T' phase involves vacancy/partial occupancy of atomic sites, and for this phase, the computed lattice parameters in Table IV correspond to the low-energy configuration/composition. (We discuss this vacancy/partial occupancy in more detail subsequently.) In general, the first-principles structural parameters in Table IV follow well-known trends: LDA values tend to underestimate experiment by ~1 to 2 pct, and GGA calculations produce systematically larger lattice constants, even overstimating experiment in cases. It is interesting to note that the *c* parameter of the π-$Al_8FeMg_3Si_6$ phase shows a more significant deviation from experiment than is typical from first-principles calculations ~5 pct and 4 pct from LDA and GGA, respectively. This discrepancy suggests either a problem with the density-functional description of this structure, or possibly a problem with the experimentally determined crystal structure.

From Table II, we see for the $Al_{12}Mn$ phase, the first-principles (GGA/LDA) heat of formation deviates from CALPHAD values by about ± 20 pct. For $Al_{13}Cr_4Si_4$, the comparison between CALPHAD and first-principles values for heat of formation is good, more typical of the comparisons we found for θ, β, and Q above. The CALPHAD heat of formation of π ($Al_8FeMg_3Si_6$) phase is -117 meV/atom for both Thermotech and Computherm databases. Interestingly, first-principles LDA and GGA calculations show a much less stable compound than this, with GGA calculation predicting a *positive* value of heat of formation for this phase, indicating its instability (at $T = 0$) with respect to phase separation of the elements. Since, for many of the other phases considered in this work, the comparison between CALPHAD and first-principles values of heats of formation were fairly reasonable, the large deviation for π ($Al_8FeMg_3Si_6$) phase between CALPHAD and first-principles indicates a possible problem with either the crystal structure or the first-principles description of this phase. It is interesting that the preceding comparison of crystal structure parameters led to the same conclusion. In several experimental works on Al-Si-Mg casting alloy, the π ($Al_8FeMg_3Si_6$) phase is observed both in as-cast and heat-treated microstructures. However, this phase is observed to decompose upon solution treatment of the low Mg alloys releasing Mg into solution and giving way to the formation of β-AlFeSi and Mg_2Si phases.[22, 35–39] It should further be noted that while the calculation of 356 alloy shows the presence of π ($Al_8FeMg_3Si_6$) phase over a narrow temperature window with both the databases, for 6022, only, Computherm results predict the presence of π ($Al_8FeMg_3Si_6$) phase. In order to verify the temperature dependence of the stability of π, CALPHAD equilibrium phase fraction calculations were performed with both databases at the precise stoichiometry of the π ($Al_8FeMg_3Si_6$) phase. It is seen in these calculations again that π ($Al_8FeMg_3Si_6$) is stable only over a narrow temperature window, and dissociates into β-AlFeSi and Mg_2Si phases upon decreasing temperatures. It is interesting that this experimental observation of the decomposition of π, the CALPHAD prediction of its decomposition at low temperatures, and the first-principles (GGA) prediction of positive heat of formation all indicate instabilities in this structure. However, given the discrepancies between first-principles, CALPHAD, and experimental values of ΔH and the lattice parameters, we assert that further experimental investigation of this phase would be of interest.

Table IV. First-Principles Calculated and Experimental Structural Information for Al Intermetallics*

Phase	Space Group; Pearson Symbol	Lattice Parameters (Å)		
		LDA	GGA	Experiment[34]
$Al_{12}Mn$	*Im*-3; *cI*26	7.35	7.47	7.47
$Al_{13}Cr_4Si_4$	*F*-43*m*; *cF*84	10.73	10.91	10.92
$Al_8FeMg_3Si_6$ (π)	*P*-62*m*; *hP*18	6.65 7.51	6.75 7.63	6.63 7.94
$Al_4Cu_4Zn_1\square^F$ (T' or τ)	*R*3; *hR*9	8.63 $\alpha = 27.32$	8.82 $\alpha = 27.38$	8.67 $\alpha = 27.41$

*Lattice parameters *a* are given for the cubic phases $Al_{12}Mn$ and $Al_{13}Cr_4Si_4$, whereas for the hexagonal $Al_8FeMg_3Si_6$ (π) phase, we list both *a* and *c*, and for the rhombohedral $Al_4Cu_4Zn_1\square^F$ (T' or τ), the lattice parameter *a* and rhombohedral angle α are given.

Al-Cu-Zn T′ phase

The T' phase is observed in Al-Cu-Zn alloys over wide composition and heat-treatment ranges.[40] Through X-ray and electron diffraction patterns, the crystal structure of T' phase has been determined to be trigonal (or rhombohedral), with lattice constant $a = 8.676$ Å with $\alpha = 27.41$ deg.[40] The unit cell of T' phase is a bcc superstructure containing ten atomic sites, placed at equal intervals along [111], i.e., at sites [*x*, *x*, *x*], with $x = 0.0, 0.1, 0.2, 0.3, 0.4, 0.5, 0.6, 0.7, 0.8$, and 0.9, labeled A, B, C, D, E, F, G, H, I, J respectively. The structure has been experimentally determined to consist of an array of Al and Cu atoms arranged alternatively along [111] with a vacancy (□) at the center of the cell (site F), which would have otherwise been occupied by the Cu atom.[40] Electron probe analysis of the T' phase indicates that Zn replaces Al in the structure.

To help elucidate the energetics of the T′ phase, as well as the energetic effects of vacancy and Zn substitution in the structure, we perform total energy calculations of the T′ phase for the following atomic arrangements:

(1) $Al_5Cu_4\square^F$,
(2) $Al_4Cu_4Zn_1\square^F$,
(3) $Al_4Cu_5Zn_1$, and
(4) $Al_5Cu_4Zn_1^F$.

The composition $Al_5Cu_4\square^F$ corresponds to a distribution of Al and Cu atoms on the two sublattices of the T' phase with a vacancy at the center of the cell (site F). The $Al_4Cu_4Zn_1\square^F$ composition corresponds to the distribution of Al and Cu atoms on the two sublattices with Zn substituted at either of the two Al lattice sites nearest to the central site F of the unit cell, and with the central site remaining vacant. The composition $Al_4Cu_5Zn_1$ is derived in the same way, except that the central vacancy site is also now occupied by Cu. We also considered another composition, $Al_5Cu_4Zn_1$, in which Zn is substituted at the central site. Thus, the last two configurations do not involve any vacancies in the structure.

In Table V, formation enthalpies of the T' phase for the various configurations are shown. Although one cannot directly and quantitatively compare ΔH values of phases with differing stoichiometries, we can still obtain some qualitative insight into the effects of various site substitutions from these calculations: By comparing GGA values of ΔH (LDA values show the same trends) for $Al_5Cu_4\square^F$ (-167 meV/atom) with $Al_4Cu_4Zn_1\square^F$ (-171 meV/atom), we see that the introduction of Zn into the structure lowers the formation enthalpy very slightly. Also, by comparison of $Al_4Cu_5Zn_1$ (-148 meV/atom) with $Al_4Cu_4Zn_1\square^F$ (-171 meV/atom), we see that incorporating a vacancy on the F site lowers the formation enthalpy more significantly. Finally, by comparing $Al_4Cu_5Zn_1$ (-148 meV/atom) with $Al_5Cu_4Zn_1^F$ (-55 meV/atom), ΔH is lower with Zn on the Al site than on the central Cu F site. Again, we reiterate that because these structures all possess different stoichiometries, a direct comparison of formation enthalpies cannot give qualitative values of the defect energies (*e.g.*, vacancy formation energy, *etc.*). To get these values of the defect energies, one would also need to consider the reference state of the substituted and replaced atom in the structure. However, from our calculations, we can say that the lowest formation energy we found was for $Al_4Cu_4Zn_1\square^F$, which is precisely the experimentally observed structure and stoichiometry.[40]

The first-principles formation enthalpy of low-energy configuration T' ($Al_4Cu_4Zn_1\square_1^F$) phase is -171 meV/atom for GGA, which is about 25 pct higher that the CALPHAD-Computherm value. It should be noted that the Computherm heat of formation of T′ phase corresponds to a composition of $Al_5Cu_4Zn_1$, which deviates from the first-principles and experimental low-energy composition of $Al_4Cu_4Zn_1\square_1$. We suggest that the Computherm database gives a T' phase whose stability is overestimated with respect to first-principles values, and based on a composition which deviates from the experimental one. These observations could explain the unexpected existence of this phase in some of the CALPHAD results of the previous section.

Table V. First-Principles Formation Enthalpies of T' Phase Configurations (meV/Atom)*

Configuration	LDA	GGA
$Al_5Cu_4\square^F$	−185	−167
$Al_4Cu_4Zn_1\square^F$	−190	−171
$Al_4Cu_5Zn_1$	−172	−148
Al_5Cu_4	−69	−55

*The experimentally observed $Al_4Cu_4Zn_1\square^F$ configuration has a strongly negative formation enthalpy.

VI. CORRELATION BETWEEN CALCULATED PHASE FRACTIONS AND MEASURED YIELD STRENGTHS

In addition to Al and Si, the equilibrium phases present in the Al alloys of the Al-Mg-Si-Cu quaternary system are Al_2Cu (θ), Mg_2Si (β), and $Al_3Cu_2Mg_9Si_7$ (Q). Precursors to these equilibrium phases are present in alloys aged to peak hardness and these precursor precipitates often turn out to be effective strengthening phases. For instance, during aging of Al-Cu, the equilibrium θ phase is often preceded by a strengthening θ' precipitate phase; in Al-Mg-Si, β is preceded by β' and β'' strengthening precipitates; and in the quaternary system, Q can be preceded by a Q' phase. Thus, from the equilibrium phases predicted for the alloys of this study, we can speculate on the types of metastable precipitates that are likely to form in these alloys. We list the calculated dominant (as well as any secondary) phases present in these alloys in Table VI.

One contribution to yield strength by precipitate phases is simply due to the amount of the precipitate phase in the alloy, or the precipitate phase volume fraction. Of course, the morphology of the precipitate microstructure, the mechanism of precipitation hardening, and other factors have a significant impact on yield strength response.[5] Nevertheless, as a simple model, we wish to see whether there exists any correlation between the calculated phase fractions of equilibrium phases and the measured yield strength of respective alloys. So we have collected the measured yield strength data[5,21,41,42] for these alloys, which are plotted in Figure 8. For comparison, we also show a plot of the calculated phase fractions (Thermotech, 0 °C) of the dominant phases (Table VI) in the respective alloys.

We note that despite the gross approximations of such a simple idea, there exists a fair degree of correlation between the calculated equilibrium phase fraction and the measured yield strengths, in spite of the different phases, morphologies, mechanisms, *etc*., that must exist across this range of alloys. Thus, we assert that these types of calculations and correlations might provide in the future an avenue for simple estimates of yield strengths of new alloys.

VII. SUMMARY

We have performed a critical comparison of the Thermotech and Computherm thermodynamic databases of aluminum alloys, by calculating equilibrium solid-state phase fractions and phase diagram isothermal sections of several industrial aluminum alloys used in automotive applications: the cast alloys W319 and 356 as well as the wrought alloys 6022 and 6111. Although many of the results are consistent between the two databases, several qualitative and quantitative differences were observed, often due to the phases involving Mn, Cr, Fe, and Zn. On the other hand, thermodynamics involving only phases from the Al-Mg-Si-Cu quaternary show good agreement between the

Table VI. Phases with Strengthening Precursors Calculated to be in Equilibrium in the Al Alloys of This Study

Alloy	Dominant Phase	Secondary Phase
W319	Al_2Cu	Q
356	Q	Mg_2Si
6022	Mg_2Si	Q
6111	Q	$Al_2Cu + Mg_2Si$

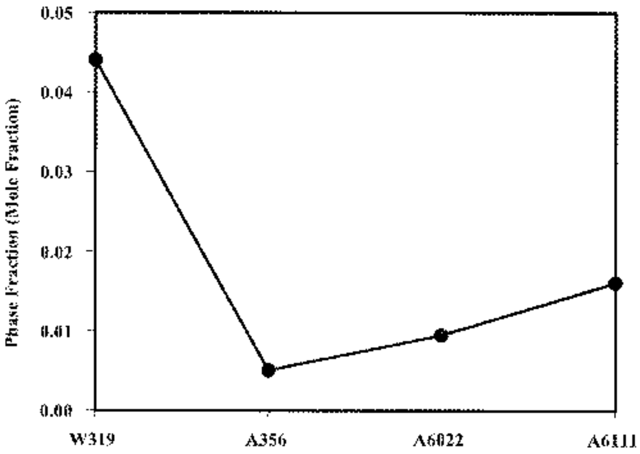

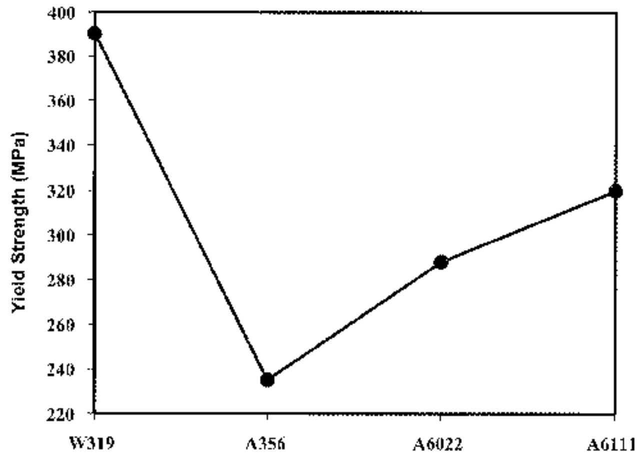

databases, although some subtle differences still exist, particularly involving the quaternary *Q* phase. To understand and assess these quantitative differences, formation enthalpies and reaction energies from the databases were compared against density functional first-principles energetics. These comparisons suggest possible avenues for future improvements of Al-alloy thermodynamic databases. Finally, we have shown that a correlation exists between the calculated phase fractions and the measured yield strengths of these precipitate-hardened alloys.

ACKNOWLEDGMENT

This work was sponsored, in part, by the National Science Foundation under Contract No. 0205232.

REFERENCES

1. L. Kaufmann and H. Bernstein: *Computer Calculation of Phase Diagrams*, Academic Press, New York, NY, 1970.
2. R. Vijayaraghavan, J.W. Zindel, and J.E. Allison: Internal Report, SRR-1999-0128, Ford Motor Company, Dearborn, MI, 1999.
3. C. Wolverton, X.-Y. Yan, R. Vijayaraghavan, and V. Ozolins: *Acta Mater.*, 2002, vol. 50, pp. 2187-97.
4. C. Wolverton and J.E. Allison: Internal Report, SRR-2001-0168, Ford Motor Company, Dearborn, MI, 2001.
5. S.C. Weakley, W. Donlon, C. Wolverton, J.W. Jones, and J.E. Allison: *Metall. Mater. Trans. A*, 2004, vol. 35A, pp. 2407-18.
6. Y. Zhong, C. Wolverton, Y.A. Chang, and Zi-Kui Liu: *Acta Mater.*, 2004, vol. 52, pp. 2739-54.
7. Y. Wang, S. Curtarolo, C. Jiang, R. Arroyave, T. Wang, G. Ceder, L.-Q. Chen, and Z.-K. Liu: *CALPHAD*, 2004, vol. 28, pp. 79-90.
8. B. Dracup, P.E.A. Turchi, V. Radmilovic, U. Dahmen, and J.W. Morris, Jr.: *Metall. Mater. Trans. A*, 2004, vol. 35A, pp. 2305-11.
9. X.J. Liu, C.P. Wang, I. Ohnuma, R. Kainuma, and K. Ishida: *Metall. Mater. Trans. A*, 2004, vol. 35A, pp. 1641-54.
10. Y. Du, J.C. Schuster, F. Weitzer, N. Krendelsberger, B. Huang, Z. Jin, W. Gong, Z. Yuan, and H. Xu: *Metall. Mater. Trans. A*, 2004, vol. 35A, pp. 1613-28.
11. T. Wang, J. Zhu, R.A. Mackay, L.-Q. Chen, and Zi-Kui Liu: *Metall. Mater. Trans. A*, 2004, vol. 35A, pp. 2313-21.
12. U.R. Kattner: *JOM*, 1997, vol. 12, pp. 14-19.
13. M. Asta, V. Ozolins, and C. Woodward: *JOM*, 2001, vol. 53, pp. 16-19.
14. J.-C. Zhao and M.F. Henry: *JOM*, 2002, vol. 54, pp. 37-41.
15. A.W. Zhu, B.M. Gable, G.J. Shiflet, and E.A. Starke, Jr.: *Adv. Eng. Mater.*, 2002, vol. 4, pp. 839-46.
16. N. Saunders, X. Li, A.P. Miodownik, and J.-P. Schille: *Light Metals, 2003*, P. Crepeau, eds., TMS, 2003, pp. 999-1004.
17. P. Donnadieu, M. Roux-Michollet, and V. Chastangnier: *Phil. Mag.*, 1999, vol. 79A, pp. 1347-66.
18. Information about the ThermoTech Al database is available on the ThermoCalc web site: http://www.thermocalc.com/Products/databas_ny/TTAl.htm. For more information on ThermoCalc, see B. Sundman, B. Jansson, and J.O. Anderson: *CALPHAD*, 1985, vol. 9, pp. 153-90.
19. Information about the CompuTherm Al database, *PanAluminum*, is available on the CompuTherm web site: www.computherm.com. For more information, see Y.A. Chang, X.-Y. Yan, S.L. Daniel, F.-Y.Xie, S.-L. Chen, and F. Zhang: *Materials Design Approaches and Experiences*, J.-C. Zhao, M. Fahrmann, and T. Pollock, eds., TMS, Warrendale, PA, 2001, pp. 85-96.
20. S.-L. Chen, F. Zhang, S. Daniel. F.-X. Xie, X.-Y. Yan, Y.A. Chang, R. Schmid-Fetzer, and W.A. Oates: *JOM*, 2003, vol. 55, pp. 48-52.
21. *Aluminum for Automotive Body Sheet Panels*, The Aluminum Association, Inc., Washington, D.C., 1998.
22. P. Friedman and C. Miller: Internal Report, SRR-2000-0085, Ford Motor Company, Dearborn, MI, 2000.
23. G. Gustafsson, T. Thorvaldsson, and G.L. Dunlop: *Metall. Trans. A*, 1986, vol. 17A, pp. 45-55.
24. R. Jahn, W.T. Donlon, and J.E. Allison: Internal Report, SRR-1999-0191, Ford Motor Company, Dearborn, MI, 1999.
25. Metals Handbook: *Properties and Selection: Nonferrous Alloys and Special Purpose Materials*, 10th ed., ASM INTERNATIONAL, Metals Park, OH, 1990, vol. 2.
26. G. Kresse and J. Hafner: *Phys. Rev.*, 1993, vol. B47, pp. 558-61.
27. D.M. Ceperley and B.J. Alder: *Phys. Rev. Lett.*, 1980, vol. 45, pp. 566-69.
28. J.P. Perdew: *Electronic Structure of Solids*, P. Ziesche and H. Eschrig, eds., Akademie Verlag, Berlin, 1991, vol. 11.
29. C. Wolverton and V. Ozolins: *Phys. Rev. Lett.*, 2001, vol. 86, pp. 5518-21.
30. C. Ravi and C. Wolverton: *Acta Mater.*, 2004, vol. 52, pp. 4213-27.
31. C. Wolverton: *Acta Mater.*, 2001, vol. 49, pp. 3129-42.
32. COST 507: *Thermodynamic Database for Light Metal Alloys*, I. Ansara, A.T. Dinsdale, and M.H. Rand, ed. European Commission, rue de la Loi 200 (SOME 1/44), July 1998, vol. 2, B-1049.
33. H. Feufel, T. Godecke, H.L. Lukas, and F. Sommer: *J. Alloys Compounds*, 1997, vol. 247, pp. 31-42.
34. W.B. Pearson, P. Villars, and L.D. Calvert: *Pearson's Handbook of Crystallographic Data for Intermetallic Phases*, ASM, Metals Park, OH, 1985.
35. J.G. Barlock and L.F. Mondolfo: *Z. Metallkd*, 1975, vol. Bd. 66, pp. 605-11.
36. S. Murali, K.S. Raman, and K.S.S. Murthy: *Mater. Sci. Eng.*, 1992, vol. A151, pp. 1-10.
37. J.A. Taylor, D.H. St John, J. Barresi, and M.J. Couper: *Mater. Sci. Forum*, 2000, vols. 331-337, pp. 277-82.
38. Q.G. Wang and C.J. Davidson: *J. Mater. Sci.*, 2001, vol. 36, pp. 739-50.
39. X. Cao and J. Campbell: *Metall. Mater. Trans. A*, 2004, vol. 35A, pp. 1425-35.
40. S. Murphy: *Met. Sci.*, 1975, vol. 9, pp. 63-168.
41. C.C. Engler-Pinto Jr., J.V. Lasecki, J.M. Boileau, and J.E. Allison: Report No. 2004-01-1029, SAE International, 2004, Detroit.
42. J.M. Boileau, C.A. Cloutier, L.A. Godlewski, P.A. Reeber-Symanksi, C. Wolverton, and J.E. Allison: SAE International Report No. 2003-01-0822, SAE International, 2003, Detroit.